Analysis of Clothing Pressure on the Human Body in Motion

Takaya Kobayashi, Yasuko Mihara

Mechanical Design & Analysis Corporation

Yumiko Isogai, Sonoko Ishimaru, and Chisato Nonomura

TOYOBO Co., Ltd.

Abstract: *In a previous study, the authors presented the development of knitted fabric models for finite element analysis to simulate the large deformation behavior of garments and the distribution of clothing pressure on the human body in a stationary position. This paper describes an extension of the investigation to a study of the human body in motion. The study accomplished a fully automatic simulation of the clothing pressure change in T-shirts during jogging. The analysis technique is expected to be utilized in the development of a stabilized electrocardiogram measurement for a person during exercise.*

Keywords: *Knitted Fabric, Shell, Buckling, Rebar, UMAT.*

1. Introduction

The comfort provided by clothes is a key element that directly affects the human psychology as well as physiology in all environmental conditions. The primary elements that compose comfort include the temperature and humidity conditions inside the clothes, which are referred to as the *micro-climate within clothing*: the pressure generated when clothing contacts the human body; and the feeling of the clothing, which is largely influenced by the materials. Among these elements, clothing pressure can be applied to improve exercise skills, reshape the body, and exert a favorable influence upon the autonomic nervous and circulatory systems for medical applications. In order to realize moderate clothing pressure, the most common approach in the sewing process is to modify the sewing repeatedly based on the examinees' sensory impressions. However, if subtle designs are required, this process may not be a highly efficient way to improve clothing.

To measure clothing pressure, sensing elements are commonly inserted between the human body and the clothes. However, practical measurements are often restricted by the available sizes of the pressure sensors and the available measuring points on a human body. Therefore, mapping the clothing pressure distribution over the entire surface of a human body remains difficult. Even if pressure data is obtained, it may not good enough to cover the design of the clothes. Since the interaction effects between the human body and clothes, for example, wrinkles, slackness, and tightness, cannot be evaluated only from the clothing pressure data, further information about the deformation of the clothes is necessary.

Recent innovations in cloth materials enable us to utilize the kinematic interaction between the human body and clothes to improve both wearing comfort and mobility function. Especially in high-value-added application fields, such as sports and medical services, the demand for better clothing is greatly increasing. For consumer products, such as underwear, the cascading effect from this high technology has broad applications and uses for direct benefits that improve daily life. In response to the recent trends, the authors sought an efficient technique for predicting the process of clothing the simulated human body using finite element analysis. In order to simulate the process, it is necessary to represent the deformation behavior of the fabric in terms of available material models. Cloth materials are complicated products made from a spinning, weaving, or knitting process. Instead of modeling the yarns, the macroscopic deformation of the yarns can be determined after they are knitted into clothing. Either way, they present their complex behavior due to the combined effects of their highly nonlinear and anisotropic properties.

In a previous study, the authors presented two analytical approaches: a rebar layer model combined with isotropic hyperelastic shell elements (Ishimaru et al. 2010, Kobayashi et al. 2011), and an anisotropic hyperelastic material model with a polyconvex strain energy function defined by the user subroutine UMAT in Abaqus (Tanaka et al. 2010). This paper describes an extension of the investigation to a study of a moving human body. Abaqus, the general purpose FEM code, is used for its powerful nonlinear analysis capability to overcome the difficulties of the material modeling and the large deformation of the clothing (Dassault 2013, Tarriera et al. 2010). The study accomplished a fully automatic simulation of the clothing pressure changes in T-shirts during jogging. The analysis technique was applied to a stabilized electrocardiogram measurement for a person during exercise.

2. Formulation of rebar layer model for knitted fabric

Cloth materials are generally classified into woven or knitted fabrics. In this study, knitted fabric with a more complicated structure is the target (Figure 1). The knitted fabric has a fiber structure with yarns mutually twined into loops. The respective directions of the wale and course are determined according to the orientation of the yarns. Figure 2 shows the deformed shapes of the actual knitted fabric stretched in the direction of the course. In the initial stage, the loops are deformed, and in the latter stage, the yarns are elongated. Consequently, it can be assumed that the measured load increment will increase gradually as the yarn is stretched. Therefore, the respective stiffness along each orientation is governed by the knitting pattern. It is common that the relationship between the measured load and the displacement shows anisotropic behavior. In this study, the nonlinearity and anisotropic characteristics exhibited by knitted fabrics are modeled with a rebar layer model.

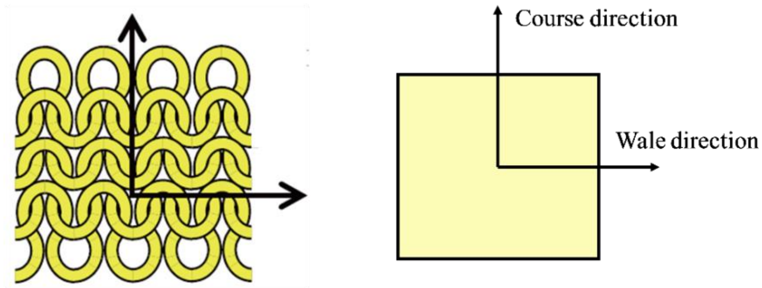

Figure 1. Schematic model of knitted fabric.

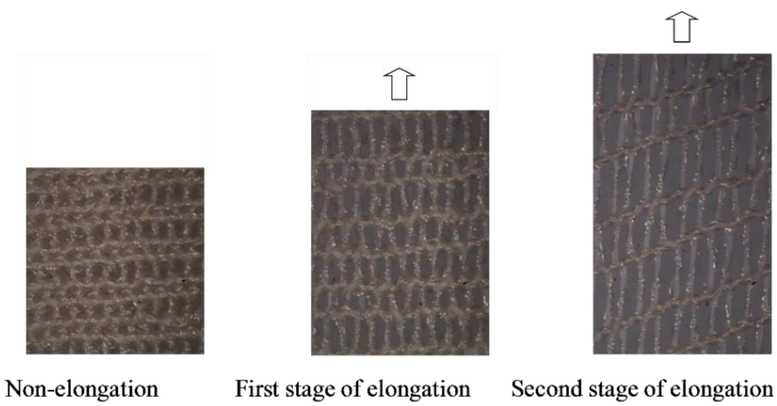

Figure 2. Elongation of knitted fabric.

The rebar layer model was built using an isotropic hyperelastic shell element for the matrix of the cloth material, combined with a rebar layer defined on the matrix along the wale and course (Figure 3) (Ishimaru et al. 2010). The isotropic matrix follows the neo-Hookean hyperelastic material model. The potential energy of the neo-Hookean hyperelastic model W_{neo} is expressed as

$$W_{neo} = C_{10}(\lambda_1^2 + \lambda_2^2 + \lambda_3^2) \quad (1)$$

where C_{10} is the material parameter and $\lambda_i \ (i = 1, 2, 3)$ represents principal stretch ratios. The first strain invariant I_1 is equivalent to $\lambda_1^2 + \lambda_2^2 + \lambda_3^2$. An element-based rebar layer is defined as the reinforcing member arranged in the specified in-plane orientation of the shell element. The rebars represent the uniaxial reinforcement along the wale and course (Figure 3). The material properties of the rebars are given by the hypoelastic model with Young's moduli of E_{wale} and E_{course}, which give the strain-dependent nonlinear axial stiffnesses. The elasticity tensor D_{ijkl} is obtained by the superposition of the isotropic matrix and the rebars as follows:

$$D_{ijkl} = \frac{\partial^2 W_{neo}}{\partial \varepsilon_{ij} \varepsilon_{kl}} + E_{wale} \delta_{1i} \delta_{1j} \delta_{1k} \delta_{1l} + E_{course} \delta_{2i} \delta_{2j} \delta_{2k} \delta_{2l}, \quad \{i, j, k, l\} = \{1, 2, 3\} \tag{2}$$

where directions 1 and 2 denote the wale and course directions, respectively. Direction 3 is perpendicular to the wale and the course directions, and δ_{ij} represents the Kronecker's delta. E_{wale} and E_{course} take the form of a series in terms of ε_{11} and ε_{22}, respectively.

$$E_{wale} = \sum_{i=0}^{N} c_i \varepsilon_{11}^i \tag{3}$$

$$E_{course} = \sum_{i=0}^{N} d_i \varepsilon_{22}^i \tag{4}$$

The material parameters C_{10}, c_i, N, and d_i (i = 1, …, 6) are determined through uniaxial tensile tests in three directions: wale, course, and bias. This rebar layer model is implemented via Abaqus/Standard in which the isotropic matrix part is represented by the shell element S4R. Its reinforcement is modeled with the rebar layers' capability. This provision allows the shell element to exhibit nonlinear and anisotropic elastic behavior. The shell element, as the matrix of the rebar layers, exhibits the Poisson's effect due to its isotropic hyperelasticity. Although the rebar layer model is easy to assemble, it is not suitable for more accurate fabric modeling of the interaction between the wale and the course. That is, the respective axial property of the wale and the course, defined as the reinforcing rebar, do not relate to each other. Taking this interactive effect into account, an anisotropic hyperelastic material model was proposed in our previous study (Tanaka et al. 2010) applying the strain energy function with the polyconvexity condition suggested by Schröder (2005) and Itskov (2006).

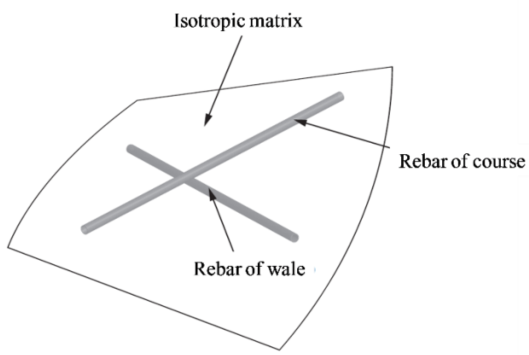

Figure 3. Schematic diagram of a shell with rebar.

3. Parameter identification of material models

To identify the material parameters, three uniaxial tensile tests are performed in three directions of wale, course, and bias (cut at a 45 degree angle), as shown in Figure 4. Figure 5 shows the results from the tensile tests made for cloth material that exhibits highly anisotropic behavior typically used for products like pantyhose and tights. Figure 5 also shows the analytical results using identified material constants. The tensile stresses in the wale and the course directions could be successfully simulated by the analysis with either of the material models (Figure 5(a) and (b)). On the other hand, the stretching along the bias shows a remarkable interaction between the wale and the course (Figure 5(c)). The deformed shape looks remarkably distorted, and higher stress is induced in the high-strain regions. As the anisotropic hyperelastic model (Tanaka et al. 2010) contains the material parameters that allow this interactive behavior, the increase in the stress can be correctly represented by this model. The rebar layer model is not capable of representing the increase in the stress because it does not take this interaction into account. The tensile test specimen is clamped at both ends, and necking deformation due to elongation is produced in the mid-portion of the test specimen. This necking reflects the interaction between the wale and the course, and therefore the analysis with the anisotropic hyperelastic model may give a better result.

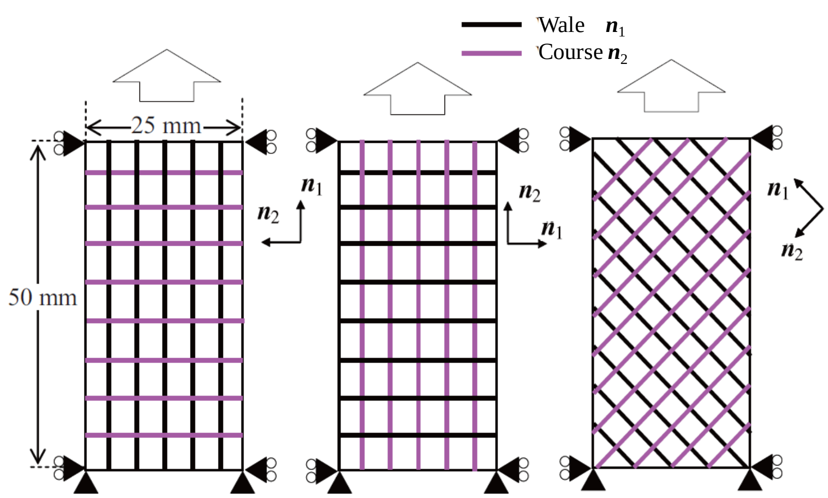

Figure 4. Simple tensile tests of knitted strips.

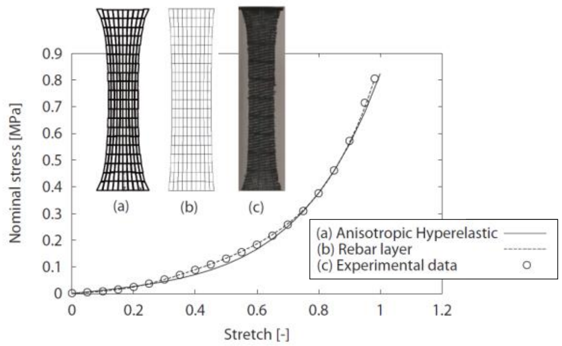

(a) Wale direction

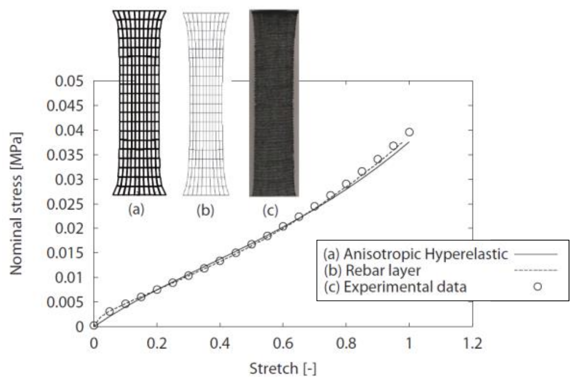

(b) Course direction

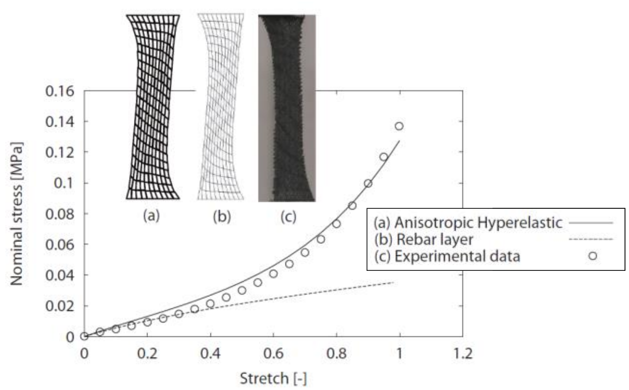

(c) Bias direction

Figure 5. Stress-strain curves of pantyhose fabric test specimen.

4. Prediction of clothing pressure for T-shirt

A three-dimensional finite element analysis was carried out using Abaqus/Standard to obtain the distribution of clothing pressure acting on a human body. The analyzed cloth is meshed with the four-node shell elements (S4R in Abaqus/Standard) and the objects chosen in this simulation were T-shirt fabrics. The material parameters of the T-shirts were determined by numerical identification for the rebar layer model. The mannequin used in this simulation corresponded to the average body of a 20-year-old Japanese woman (Figure 6). Pressure sensors were used to measure the contact pressure between the cloth and the mannequin’s surface. This experimental system served to obtain point-to-point measurement data, but such observations can hardly predict the overall distribution of contact pressure on a human body. To overcome this problem, a numerical simulation using a nonlinear FEM was conducted. In this study, the human body was modeled using rigid elements. The friction between the cloth and the human body was considered in the simulation. The Coulomb friction coefficient was assumed to be 0.8, while there are great variations for each subject.

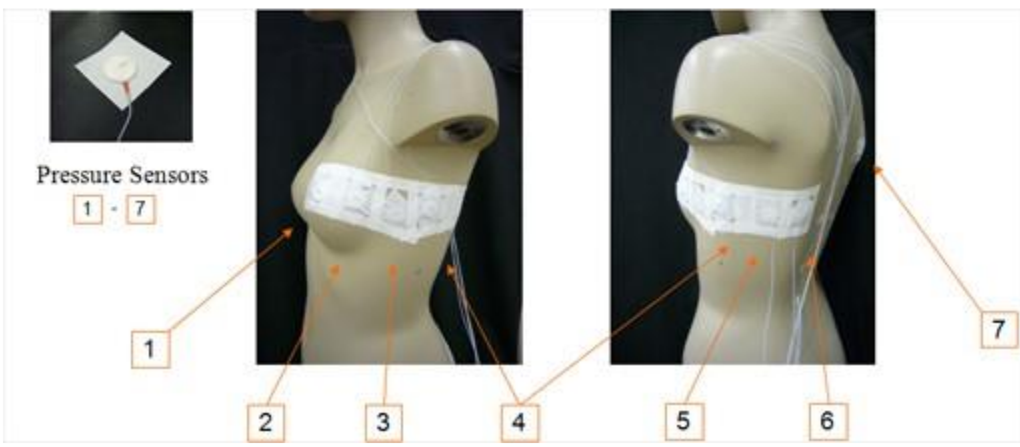

Figure 6. Measurement of clothing pressure on mannequin.

Figure 7 shows the process of clothing the simulated human body (INSIGHTS, 2009). Prior to sewing, the T-shirt was segmented into four parts: front bodice, back bodice, left sleeve, and right sleeve. Each of these parts was modeled based on geometry in accordance with the dimensions given by the respective dress pattern and was placed at the specified position around the mannequin. The simulation process progressed in such a way that the cloth parts were stretched by imposing the enforced displacement on the nodes that composed the stitch line, and each part was gently gathered to cover the surface of the mannequin. The nodes to be stitched were guided to the same position by enforced displacement so that these nodes were tied to each other. After sewing was completed, the enforced displacement imposed on each node was released so that the T-shirt began to deform to fit the surface of the mannequin and rest in a stable equilibrium state.

Figure 7 (right) shows the shape obtained in the stable state. When enforced displacement was imposed on each part, the cloth was mostly subjected to tensile stresses, but wrinkles occurred in some parts during the fitting phase. Figure 7 shows that the cloth around the waist of the mannequin was actually wrinkled. From the viewpoint of structural analysis, such deformation can be regarded as local buckling. The material model employed in this study was formulated with the constitutive law in the behavior under tension, but the stiffness against compression was set to zero. Accordingly, along with the occurrence of the local buckling, this was likely to lead to a numerical instability state. If the instability is localized (e.g., surface wrinkling or local buckling), there will be a local transfer of strain energy from one part of the model to the neighboring parts, and the conventional approach, which is typically represented by the arc-length method, may not work. This class of problems must be solved either dynamically or with the aid of artificial damping. Abaqus/Standard (Dassault 2013) provides an automatic mechanism for stabilizing unstable quasi-static problems through the automatic addition of volume-proportional damping to the model. In real cases, the energy generated by the artificial damping is equivalent to the energy released as the inertia effect. Specifically, replacing the kinetic energy with artificial damping energy makes it possible to analyze the unstable phenomenon in a stable condition in order to obtain the equilibrium solution within the static analysis.

Figure 7 (right) also shows the contact pressure. As the curvature along the back of the human body is small, the intensity of the clothing pressure is likely to be reduced and the pressure tends to concentrate on the protuberance of the shoulder blade. In the case of the shirts specifically designed for athletes, optimizing the pressure distribution was contrived by changing the cloth material from part to part. Figure 8 shows the clothing pressure distributed along the bust line. The match between the analytical results and the experimental measurements was good.

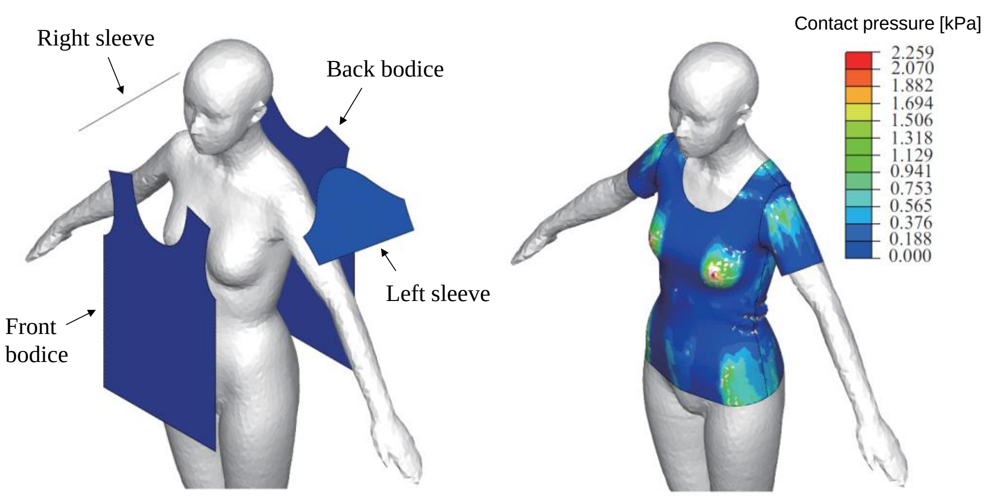

Figure 7. Process of clothing the simulated human body.

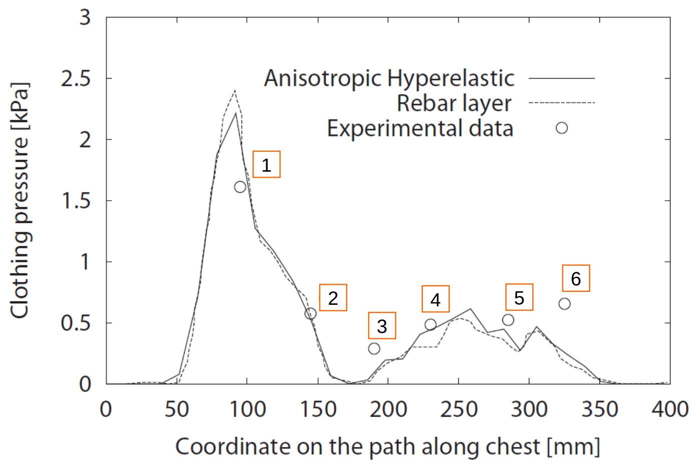

Figure 8. Clothing pressure distribution along the bust line.

5. Modeling of the Human Body in Motion

A simulation system, which represents the motion of a human body with a small amount of processing and with moderate accuracy, was developed. The system is capable of easily preparing the movement of a mannequin from the captured marker position information on the joints of a subject doing an exercise. Assuming that the mannequin is subjected to a posture change, the 3D coordinates for all the nodal points on the displaced mannequin surface were estimated from the initial shape of the mannequin and the movement of the joints. Autodesk Maya® and MotionBuilder®, the 3D animation software, were used for their practical capability of realizing the natural surface movement of the muscles of a living body from captured motion data. In this study, the analysis technique is expected to be utilized in the development of a stabilized electrocardiogram measurement on the human trunk surface for a person during exercise. It can be said from this standpoint that the macroscopic motion, twisting the upper part of the body while lifting the arm, for example, can be appropriately estimated, while the motion of the arm itself, such as the motion of the muscles around the arm joint in conjunction with large angle variations of the joint, might not be determined accurately. The resultant coordinate sets of the mannequin surface were prepared for each time step to represent the motion of the whole jogging process. Abaqus applies these coordinate data to the rigid body representation in the CONTACT option, so that the changes in clothing pressure can be calculated on the rigid human body in motion.

Figure 9 shows the dress pattern models. Two types of T-shirt patterns with different widths were examined for changes in clothing pressure during jogging. Figure 10 shows the load-stretch curves for the T-shirt test specimens. Prior to jogging, the wearing process was analyzed for the stationary position of the mannequin. After the T-shirt rested in a stable equilibrium state, the motion of the mannequin was initiated.

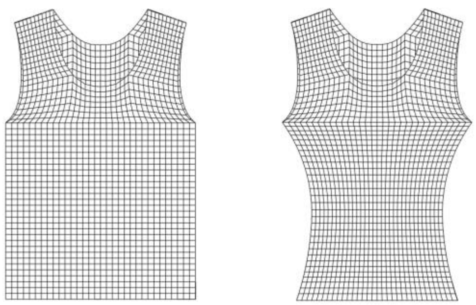

(a) Original design (b) Tight-fitting design

Figure 9. Dress pattern models for T-shirts.

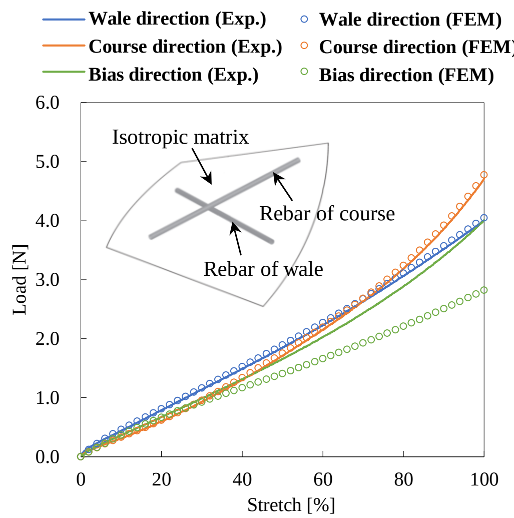

Figure 10. Load-Stretch curves for T-shirt test specimen.

The implicit dynamic response analysis (the HHT method in Abaqus) was applied to solve the jogging process. Incidentally, the explicit dynamic method is poorly suited to lengthy events (empirically more than one second). Figure 11 shows the contact pressure change for the original dress pattern (Figure 9 (a)) during jogging. The wrinkles are initiated at the right bottom portion on the back of the T-shirts, as clearly seen in step 60 in Figure 11, because the original dress pattern retains margins at the waist. The wrinkles are dislocated by the posture change of the mannequin. Figure 12 shows the contact status distribution for the original dress pattern. The contact status, which is a standard output of Abaqus, indicates whether or not the fabric is in contact with the mannequin. If the contact status is “close,” it also distinguishes whether the fabric sticks to the mannequin or slips on the surface. Based on our past investigation with clothing pressure analysis in a stationary position, the area obliquely down a shoulder blade was considered a possible location for the electrocardiogram measurement. However, as shown in Figure 12, the contact status repeats the sticking and slipping in this area due to the shift in location of the wrinkles at the waist, which would compromise an electrically stable measurement.

Figure 13 and Figure 14 show the analytical results for the tight-fitting dress pattern. Sensory tests results indicate that the maximum clothing pressure without deteriorating the comfort is around 2 kPa. However, sensitivity to comfort varies depending on regions of the human body. For example, the lower part of the trunk including the hipbone is not sensitive to tightening, while it is desirable to retain margins at the upper trunk to maintain comfort. In this study, a modified dress pattern, moderately tightening the waist, with clothing pressure not exceeding 1 kPa, was designed as shown in Figure 9(b). As shown in Figure 13 and Figure 14, the wrinkles are hardly observable and, consequently, the persistent sticking condition is achieved at the focused point for the stabilized electrocardiogram measurement.

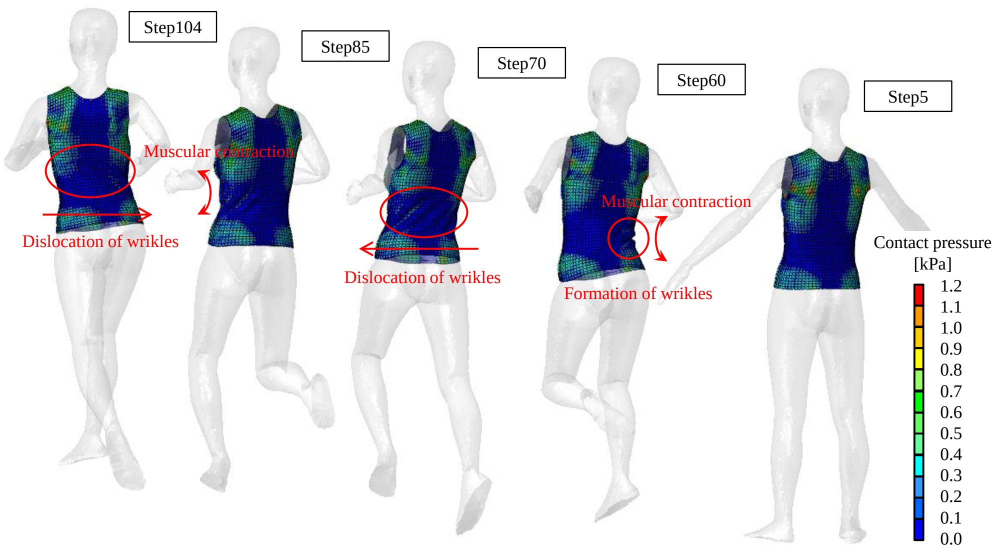

Figure 11. Clothing pressure distribution on the human body in motion (Original dress pattern).

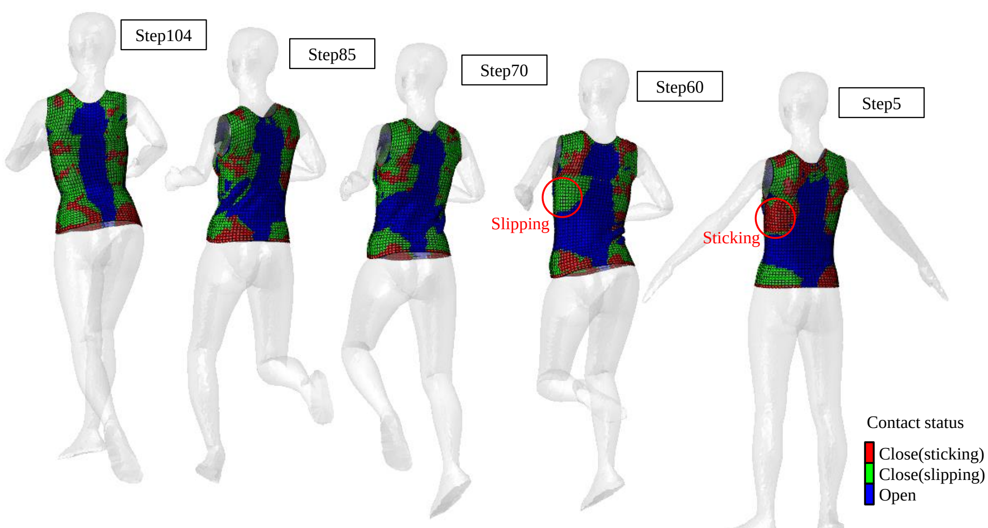

Figure 12. Contact status distribution on the human body in motion (Original dress pattern).

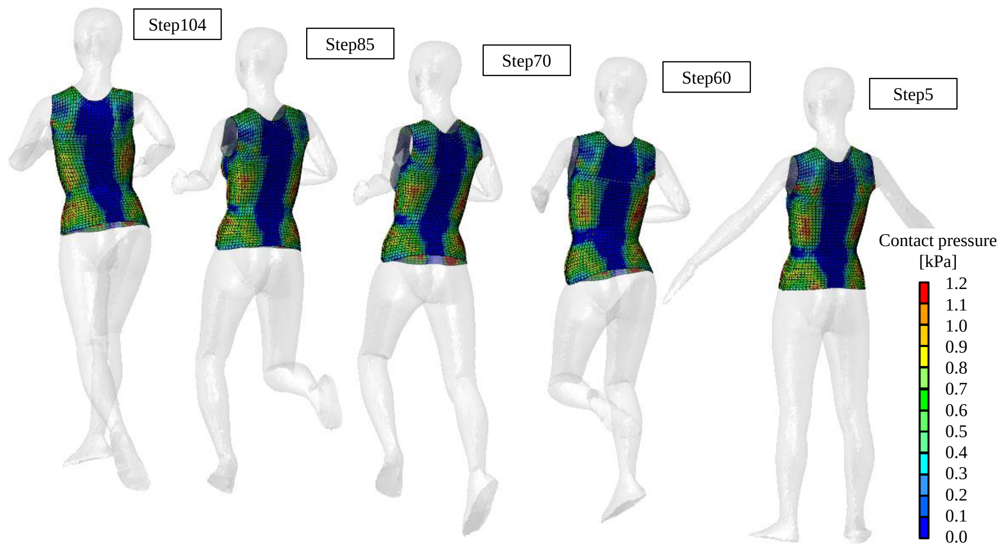

Figure 13. Clothing pressure distribution on the human body in motion (Tight-fitting dress pattern).

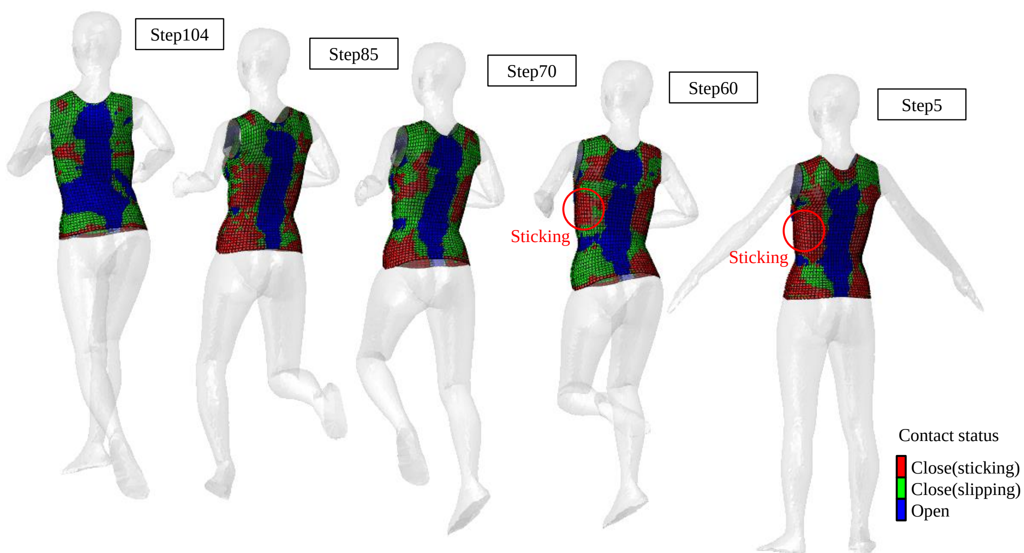

Figure 14. Contact status distribution on the human body in motion (Tight-fitting dress pattern).

6. Toyobo develops wearable material that measures heart rate

Toyobo Co., Ltd. developed a film-like functional material for clothes capable of measuring physiological information using conductive material (TOYOBO Europe, 2016, Nikkei Technology, 2015). The stretchable conductive material, COCOMI, is used for electrodes and electric wires of sensors that measure the physiological information of the wearer, and achieves both natural comfort and high-accuracy measurements. The material has the following characteristics. It features high stretchability. Whereas the authors aware that human skin can be stretched to 1.7 times its original size, this material can be stretched to roughly double its length. It is about 0.3 mm thin, and its conductive layer has high conductivity. It can be easily attached to cloth by thermo-compression bonding. When the new material is attached to clothes, it provides natural comfort similar to the comfort of normal clothes because it is thin, does not cause a height difference at the part connecting electrodes and electric wires, and is flexible enough to cope with body movements. Also, because of its high conductivity, the material is able to collect highly accurate physiological information such as weak myocardial electric signals. Using the latest finite element technology, the positions of the electrodes can be optimized to further improve accuracy, as shown in Figure 15. Toyobo plans to apply the new material and clothes to sportswear and to use them for medical purposes.

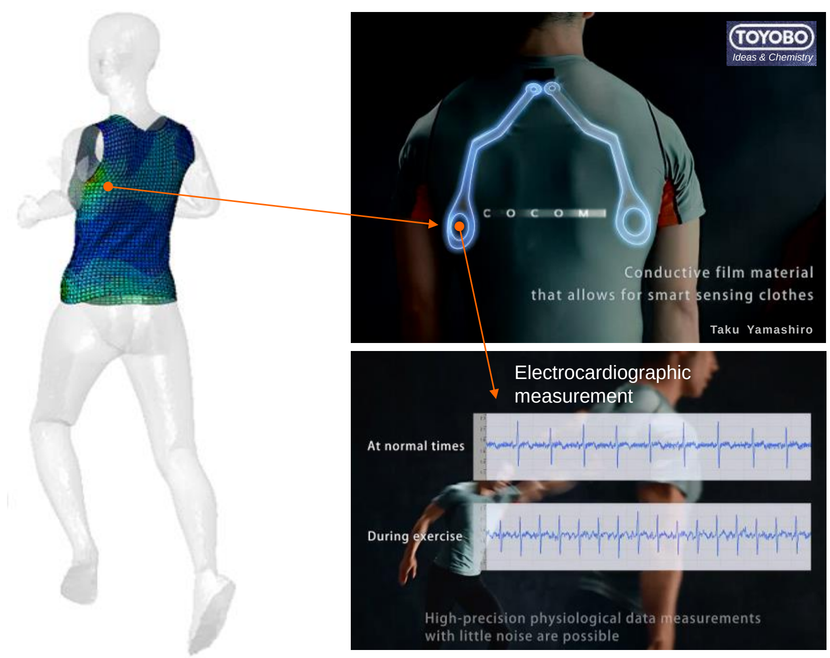

Figure 15. Stretchable conductive material COCOMI for electrocardiogram measurement.

7. Conclusion

This study presents the implementation of a material model to predict the mechanical behavior of cloth. The rebar layer model consisted of an isotropic hyperelastic matrix part and a reinforcing rebar layer part. The simulation successfully computed the pressure exerted by clothing on a mannequin, and good agreement with the experimental data was realized. The analysis technique was expanded to the prediction of clothing pressure changes on the human body in motion. The study was applied to a stabilized electrocardiogram measurement for a person during exercise.

8. References

1. Dassault Systems Simulia Corp.: Designing COMFORT into clothing, INSIGHTS, May/June 2009, 16-18, 2009.
2. Dassault Systems Simulia Corp., Abaqus Users Manual, Version 6.13, USA, 2013.
3. Ishimaru, S., Isogai, Y., Matsui, M., Furuichi, K., Nonomura, C., and Yokoyama, A., Prediction method for clothing pressure distribution by numerical approach: Attention to deformation by the extension of knitted fabric, Textile Research Journal, 81-18, 1851-1870, 2011.
4. Itskov, M., Ehret, A. E., and Mavrilas, D., A polyconvex anisotropic strain energy function for soft collagenous tissues, Biomech Model Mechanbiol, 5, 17-26, 2006.
5. Kobayashi, T., Oi, S., Sato, M., Tanaka, M., Isogai, Y., Furuichi, K., Ishimaru, S., and Nonomura, C., Analysis of Clothing Pressure on the Human Body, 2011 SIMULIA Community Conference, May 17-19, 2011, Barcelona, Spain.
6. Nikkei Technology, Toyobo Develops Wearable Conductive Film, Kojima, I., Aug 18, 2015, http://techon.nikkeibp.co.jp/english/NEWS_EN/20150818/432081/
7. Schröder, J., Neff, P., and Balzani, D., A variational approach for materially stable anisotropic hyperelasticity, International Journal of Solids and Structures, 42, 4352–4371, 2005.
8. Tanaka, M., Noguchi, H., Fujikawa, M., Sato, M., Oi, S., Kobayashi, T., Furuichi, K., Ishimaru, S., and Nonomura, C., Development of large strain shell elements for woven fabrics with application to clothing pressure distribution problem, CMES, 62-3, 265-290, 2010.
9. Tarriera, J., Harlanda, A., Jonesa, R., Lucasb, T., and Price, D., Applying finite element analysis to compression garment development, 8th Conference of the International Sports Engineering Association, 2010.
10. TOYOBO Europe GmbH, COCOMI Product Spec, https://www.youtube.com/watch?v=2qcLJkoY5XE, 2016.